Swarm and Evolutionary Computation 57 (2020) 100710

Contents lists available at ScienceDirect

Swarm and Evolutionary Computation

journal homepage: www.elsevier.com/locate/swevo

Optimization of Lennard-Jones clusters by particle swarm optimization with quasi-physical strategy

Guizhen Mai [a], Yinghan Hong [b,*], Shen Fu [c], Yingqing Lin [d], Zhifeng Hao [e], Han Huang [c], Yuanhao Zhu [d]

[a] School of Computer Science and Technology, Guangdong University of Technology, Guangzhou, 510006, China
[b] School of Physics and Electronic Engineering, Hanshan Normal University, Chaozhou, 521041, China
[c] School of Software Engineering, South China University of Technology, Guangzhou, 510006, China
[d] School of Applied Mathematics, Guangdong University of Technology, Guangzhou, 510520, China
[e] School of Mathematics and Big Data, Foshan University, Foshan, 528000, China

ARTICLE INFO

Keywords:
Particle swarm optimization
Quasi-physical strategy
Multimodal global optimization
Lennard-Jones (LJ) clusters

ABSTRACT

The goal of Lennard-Jones (LJ) clusters optimization is to find the minimum value of the potential function of a cluster and thereby determine the stable configuration of the cluster. It is essentially a completely inseparable multimodal global optimization problem, and using the traditional particle swarm algorithm to solve it often results in local convergence, which means that the solution accuracy of the algorithm is not high. Thus, in this study, we develop a LJ algorithm using a particle swarm optimization (PSO) method and a physical approach to improve the solution accuracy. In this quasi-physical strategy (QPS), the particle swarm algorithm is used to simulate the real atomic structure and incorporates the interatomic force to construct a convergence model so that the algorithm performs well in both global and local space. The potential energy functions of a variety of LJ cluster systems are selected as test functions, and the improved PSO algorithm (QPS-PSO) is analyzed and compared with a competitive swarm optimizer, cooperative coevolution PSO, and differential-group cooperative coevolution, variable-length PSO for feature selection, heterogeneous comprehensive learning PSO, ensemble PSO and cooperative coevolution with differential optimization. The results show that the PSO algorithm for LJ clusters using the proposed QPS has noticeably superior solution accuracy, especially in high-dimensional spaces.

1. Introduction

Clusters are relatively stable aggregates of a few to several thousand atoms that are formed by physical and chemical bonding and thus constitute a distinct form of substance. Unlike monomers, the physical or chemical properties of clusters often change with the number of atoms or molecules contained in the cluster. These characteristics give clusters an important role in the development of new materials such as energy storage, superconductivity, photocatalytic water-cracking and high-pressure structures [1].

At present, there are many methods of studying cluster theory, most of which use empirical potential to describe the interactions between atoms or molecules. For example, the Lennard-Jones (LJ) clusters [2] model is a very precise cluster model for inert gases, and it has been widely studied. As the minimum value of the cluster potential energy usually corresponds to the stable structure of the ground state of the cluster, the optimization of the cluster structure also serves as a prediction of the minimum-energy structure of the cluster [3]. However, the number of local minima of the potential function increases exponentially with the increasing cluster size, and therefore, optimizing the cluster structure has been proven to be a *NP*-Hard problem [4]. For such problems, it is impossible to find an effective algorithm with polynomial-time complexity [5]. In addition, as a large-scale global optimization problem, the potential function is completely inseparable. Therefore, our research goal is to design an effective optimization algorithm to solve the problem of cluster optimization.

To date, many methods have been proposed to optimize the cluster structure [6]. These can be classified as biased and unbiased methods. Most of the methods used to solve atomic structure optimization have deviations; that is, the basic configuration of the cluster needs to be preset, such as by a static lattice search [7], configuration seed algorithms and similar techniques. These can reduce the difficulty of cluster

* Corresponding author.
E-mail address: honyinghan@163.com (Y. Hong).

https://doi.org/10.1016/j.swevo.2020.100710
Received 29 May 2019; Received in revised form 8 May 2020; Accepted 10 May 2020
Available online 18 May 2020

optimization, but they are only applicable to specific clusters and are difficult to be applied to the same feature optimization problems, which significantly limits their utility.

Unbiased methods such as genetic algorithm (GA) [8], particle swarm optimization (PSO) [9,10], simulated annealing algorithm (SA) [11,12] and immune optimization algorithm (IOA) [13] have been increasingly applied in cluster structure optimization. These methods do not require a preset initial configuration, but the objective function and gradient need to be solved; these methods are commonly used to optimize clusters with different numbers of atoms and in optimization problems with the same characteristics. At the same time, as cluster optimization is a global optimization problem with large-scale and multimodal characteristics, the use of heuristic algorithms to solve the same cluster structure optimization problems is of great interest.

In recent years, PSO has been successfully applied in many research fields, such as structural prediction. PSO was proposed by Kennedy and Eberhart in the mid-1990s [14]; it is a stochastic global optimization algorithm with simple rules, few adjustable parameters, easy implementation, and fast convergence [15]. However, as the number of local minima of LJ clusters functions increases exponentially with cluster size and the different dimensions of LJ clusters functions are completely inseparable, PSO often struggles to adopt cooperative coevolution with differential grouping (CC) [16] and the divide-and-conquer (DC) [17,18] strategy, and thus it falls into a local optimum. Recently, Binh Tran proposed a length-variation mechanism that sorted the characteristic attributes of a particle swarm and focused the search on a smaller and more useful area, which improved the performance of the algorithm to some extent. However, in the mechanism of length variation, some phase information for high dimensions is inevitably lost, which is affecting the performance of the algorithm to some extent [19].

To prevent above, a quasi-physical strategy (QPS) is embedded in PSO, creating a QPS-PSO approach to solving the optimization problem of LJ clusters. To simulate the interaction between atoms in PSO, the QPS is designed to drive particle motion, and an approach that uses physical properties to construct the two convergence operation modes of the QPS is adopted as the local search method. In this QPS framework, the attraction operation helps the particle swarm find the local minimum, and the repulsion operation helps the particle swarm exit the local minimum, thus improving the performance of the PSO algorithm in solving the LJ clusters optimization problem. To test the performance of the proposed QPS-PSO algorithm for LJ clusters structure optimization with multimode and large-scale characteristics, the seven most advanced existing algorithms are compared with it.

This paper is organized as follows: Section 2 describes the LJ clusters optimization problem. Section 3 proposes the details of the proposed evolutionary algorithm. Section 4 describes the experimental analysis and results by comparing the proposed algorithm with other approaches in the literature. Section 5 concludes the paper.

2. The LJ clusters optimization problem

The LJ clusters optimization problem can be summarized as the problem of finding one of the most stable structures of a cluster in three-dimensional Euclidean space, where the number N of atoms of a cluster and the type of each atom are known. Based on theoretical predictions, chemists generally accept that the global minimum solution on a potential surface of the cluster corresponds to the geometry of the cluster [6]. Therefore, the aim of converting the problem of cluster structure prediction into a mathematical global optimization problem is to obtain the lowest potential energy of the cluster.

The LJ potential function is at the core of LJ clusters optimization and is widely used to model the behavior of noble gases in theoretical chemistry [20]. The LJ potential function is simple in form, relying only on the distance between atoms related by a 12-6 pair potential. The relevant equations are given below, beginning with Equation (1):

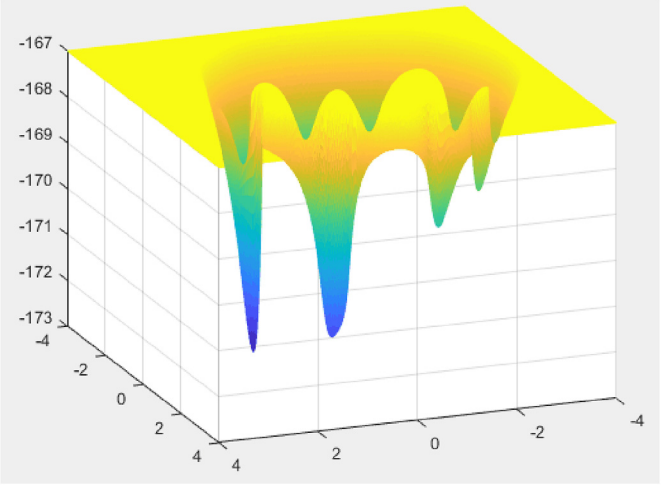

Fig. 1. The fitness function landscape above two dimensions of 38 atoms (114 dimensions).

Table 1
LJ clusters and the corresponding number of local minima (approximately equal).

Number of Atoms	Number of Local Minimum
6	2
7	4
8	8
9	21
10	57
11	145
12	366
13	988
15	10^4
25	10^6
55	10^{10}
100	10^{40}
147	10^{60}

$$v_{ij} = \left(\frac{\sigma}{r_{ij}}\right)^{12} - \left(\frac{\sigma}{r_{ij}}\right)^{6} \tag{1}$$

where v_{ij} denotes the potential energy between the i-th and j-th atoms andr_{ij} is the Euclidean distance between the coordinates of vectors x_i and x_j, where x_i is the coordinate of the i-th particle. The potential energy E_{LJ} of the cluster is given by Equation (2) as follows:

$$E_{LJ} = 4\varepsilon \sum_{i} v_{ij} \tag{2}$$

$$E_{LJ} = 4\varepsilon \sum_{i=1}^{N-1} \sum_{j=i+1}^{N} \left[\left(\frac{\sigma}{r_{ij}}\right)^{12} - \left(\frac{\sigma}{r_{ij}}\right)^{6} \right] \tag{3}$$

where N is the number of atoms, such that ε and σ are the pair well depth and equilibrium pair separation. The LJ clusters in this study were selected with the simple form $\varepsilon = \sigma = 1$ [21]. According to Equation (3), the optimization of the LJ clusters structure is essentially an unconstrained continuous optimization problem.

Although the surface form of the potential function of LJ is simple, the potential surface of LJ is rough [22]. As shown in Fig. 1, the fitness function image of more than 38 atoms in two dimensions is a double-funnel type and has many local minima; it is easy to fall into one of these, leading to local optimal or premature convergence [23]. Moreover, as a large-scale global optimization problem, the function of LJ clusters is fully non-separable. The number of local minima with respect to a cluster's potential energy tends to grow exponentially with

cluster size. Thus, Hoare supposed that for an LJ clusters of N particles, the number of minima is $O(e^{N^2})$ [24]. As shown in Table 1, when $N = 13$, the LJ problem has 988 local minimum points, and when $N = 100$, it has 10^{40} local minimum points. More details of these data are listed in Table 1 [25]. In addition, the position of each atom is represented by a three-dimensional coordinate. When the number of atoms becomes large, the structure prediction becomes a large-scale optimization problem, and each dimension is completely independent.

Above all, the optimization of the LJ clusters problem is an unconstrained large-scale multimodal optimization problem. When the number of atoms is large, the problem is very difficult to solve.

3. The proposed optimization algorithm

3.1. Particle swarm optimization

PSO is a global random search algorithm based on swarm intelligence. In the n-dimensional solution space, PSO first initializes a particle swarm batch containing m particles, where m is the particle swarm size. The coordinates of each particle represent a possible solution, and the particle coordinates play a role in determining the fitness value calculated by the objective function. In each iteration, a particle can find its own optimal solution (individual extreme value Pbest) and the optimal solution of the entire particle swarm (global extreme value Gbest) through the adaptive value to update its speed and position.

The mathematical descriptions of the PSO algorithm are as follows:

$X_i = (X_{i1}, X_{i2,\ldots,} X_{in})^T$ is the coordinate of the i-th particle in the n-dimensional solution space.

$V_i = (v_{i1}, v_{i2,\ldots,} v_{in})^T$ is the velocity of the i-th particle in the n-dimensional solution space.

The optimal position searched for the i-th particle is $P_i = (P_{i1}, P_{i2,\ldots,} P_{in})^T$.

The optimal position searched by the whole particle swarm is $G_i = (G_{i1}, G_{i2,\ldots,} G_{in})^T$.

Furthermore, the particles update their speed and position according to Equations (4) and (5).

$$v_{id}^{k+1} = \omega \cdot v_{id}^{k} + c_1 \cdot r_1 \left(p_{id}^{k} - X_{id}^{k}\right) + c_2 \cdot r_2 \left(g_{id}^{k} - X_{id}^{k}\right) \tag{4}$$

$$X_{id}^{k+1} = v_{id}^{k} + X_{id}^{k} \tag{5}$$

where $i = 1, 2, 3\ldots, n$ is the number of particles; $k = 1, 2, \ldots, n$ is the number of independent variables; d is the dimensional component of the solution space; w is the inertia weight coefficient; and c_1, c_2, r_1, and r_2 are random numbers in (0,1) respectively. In addition, p_{id}^{k} is an individual extreme position in the d dimension of particle i and g_{id}^{k} is the global extreme position of the particle swarm in the d dimension.

Then, the updated $X_i = (X_{i1}, X_{i2}, \ldots, X_{in})^T$ is decomposed into the atoms of a single LJ clusters $x_i = (x_{i1}, x_{i2}, \ldots, x_{ih})^T$, where x_{ij} represents an LJ clusters atom and h represents the number of cluster atoms. The relationship between $X_i = (X_{i1}, X_{i2}, \ldots, X_{in})^T$ and $x_i = (x_{i1}, x_{i2}, \ldots, x_{ih})^T$ is shown in Equations (6) and (7):

$$X_i = \left(x_{i1}^T, x_{i2}^T, \ldots, x_{ih}^T\right)^T \tag{6}$$

$$x_{ij} = \left(X_{i,(l(j-1)+1)}, X_{i,(l(j-1)+2)}, \ldots, X_{i,(lj)}\right)^T \tag{7}$$

where l is the dimension of a single atom x_{ij} and $n = hl$. Using these relationships, a particle in the PSO is associated with an atomic structure, which means that a particle in the algorithm contains all the position information of an atomic structure.

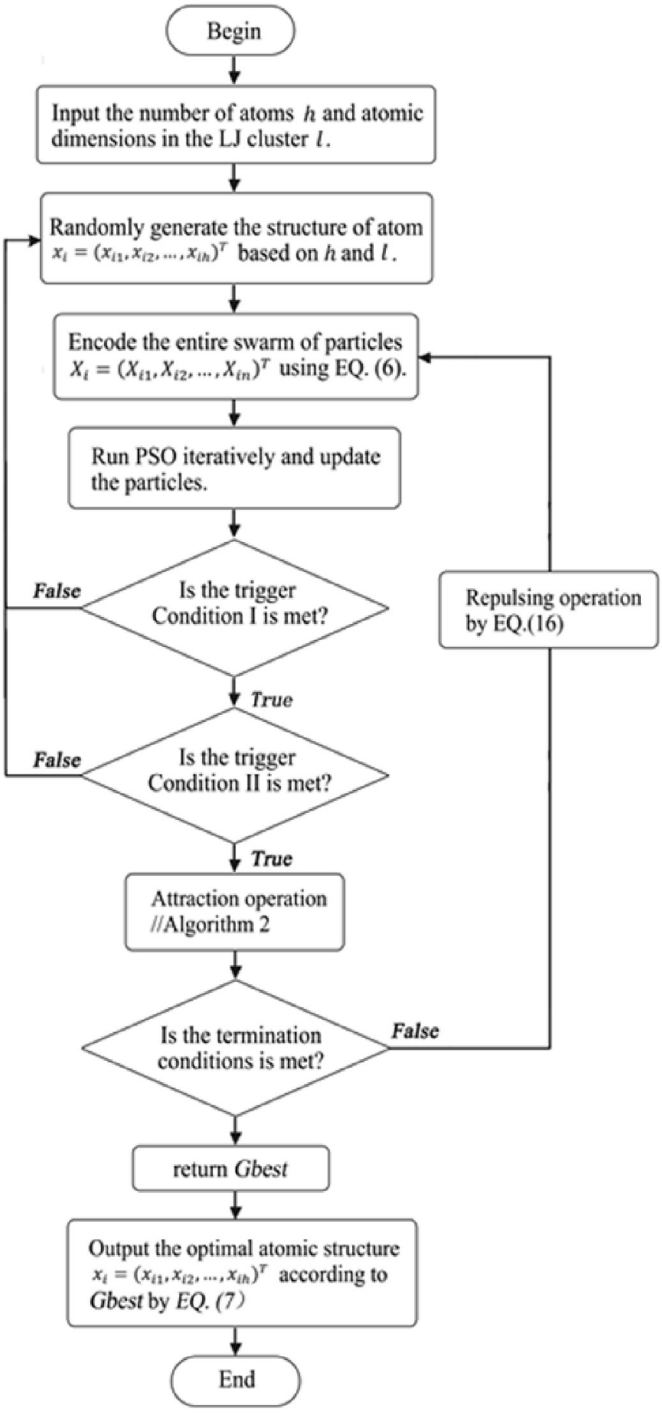

Fig. 2. Algorithm 1 flow chart for QPS-PSO.

3.2. Particle swarm optimization with a quasi-physical convergence strategy (QPS-PSO)

Although the PSO algorithm with local search can afford better search results than the PSO algorithm alone, it greatly reduces the search performance when solving high-dimensional structures. The reason for this is described in Section 2. In brief, the number of local minimum values of the cluster potential energy increases exponentially with the increase in the number of atoms in the cluster, which makes the PSO algorithm converge prematurely and fall into a local optimum. Therefore, a QPS strategy is adopted to make the particle swarm effectively converge to the global optimum.

The QPS is an algorithmic strategy with two basic operation modes, the attraction operation and repulsion operation, and two trigger conditions, denoted I and II. In this study, the algorithm embedded in QPS is designed to find the global minimum value of a LJ clusters effectively.

In this algorithm, the QPS involves iterating the PSO algorithm to verify the convergence performance of the algorithm. Using the QPS, we have two different operations to perform: the attraction operation, which helps the particle swarm to find the local minimum, and the repulsion operation, which helps the particle swarm to exit the local optimum and restart the convergence-seeking process again. The process of QPS-PSO is also shown as Algorithm 1 and the flow chart for QPS-PSO see Fig. 2.

$$|gbest_t - gbest_{t-1}| < \frac{|gbest_t - gbest_0|}{t} \tag{8}$$

Trigger condition I is calculated by Equation (8) and determines whether the quasi-physical policy is satisfied, that is, whether the change in Gbest in the last two iterations is less than the average change in Gbest over all iterations; it thereby determines whether the results converge. If condition I is met, then the iteration results converge, and the next step is carried out. If trigger condition I is not met, then the iterative process continues. Trigger condition I guarantees that the result of the algorithm's iteration is convergent [26].

Algorithm 1

QPS-PSO.

Input: the number of atoms h and atomic dimensions l in the LJ clusters.
Output: $x_i = (x_{i1}, x_{i2}, \ldots, x_{ih})^T$ optimal atomic structure after QPS-PSO
begin
  Randomly generate the structure of LJ clusters $x_i = (x_{i1}, x_{i2}, \ldots, x_{ih})^T$
  Encode the entire swarm of particles $X_i = \left(X_{i1,}X_{i2,\ldots,}X_{in}\right)^T$ using EQ. (6) and $t = 0$;
  while termination criterion is not met **do**
    $t = t + 1$
    Run PSO iteratively and update the particles;
    If $t \ mod \ \tau = 0$ **then**
      if Trigger Condition I using EQ.(8) is met then
        if Trigger Condition II using EQ.(9) is met **then**
          Run Interatomic Algorithm 2. Attraction Operation
          Run Interatomic repulsion operation using EQ.(16)
        else Trigger Condition II using EQ.(9) is not met
          Randomly initialize particle swarm
        end
      end
    end
  end
  return $Gbest'$
  Calculate x_{best} according to $Gbest'$ using EQ. (7)
end

$$\Delta r = \frac{\sum_{i=1}^{n}(pbest_i - \overline{pbest})}{n_0} < k \tag{9}$$

Trigger condition II is calculated by Equation (9), where Δr represents the mean variance in each particle in the particle swarm above each dimension, k is a constant threshold and $n_0$is the number of particles in the swarm. Trigger condition II is used to determine the degree of particle swarm aggregation. Thus, in the last iteration, the results for each particle are calculated to determine whether the variance is $< k$. If condition II is met, indicating that most particle search results are similar, the algorithm proceeds to the next step; otherwise, the iteration continues. Trigger condition II ensures the stability of the iterative results.

Trigger condition II is a judgment condition used to decide whether to perform the attraction and repulsion operations or initialize the particle swarm. If trigger condition II is met, the majority of the particles converge to a region, and in this case, the attraction operation is adopted first to help the particle swarm find the local minimum value. When the algorithm converges to a potential energy value, the result is not always global optimal, so the repulsion operation must be performed to create a large disturbance in the order, thereby slowing local convergence and enabling the particles to escape from the local optimum. If trigger condition II is not met, most particles fail to converge to a certain region within a specified number of steps, and then the particle swarm is initialized so that it exits the current convergence region and begins the convergence process again. Figs. 3 and 4 demonstrate the two cases of trigger condition II.

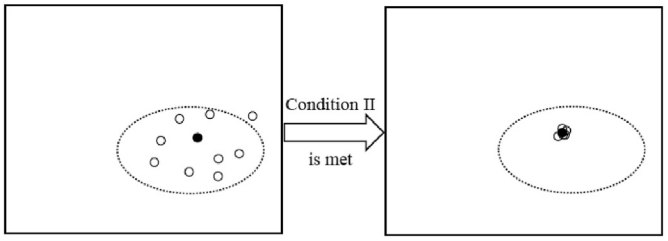

Fig. 3. The attraction operation is applied of a case which the trigger condition II is met.

3.3. The interatomic attraction operation and the interatomic repulsion operation

Structure prediction is a practical problem in physics, so we can use physical properties to define two kinds of convergence. The proposed QPS-PSO adopts a quasi-physical strategy as a local search method for the attraction operation and repulsion operation [27]. The primary utility of a quasi-physical algorithm lies in its ability to transform abstract problems into real problems, thereby enhancing their natural solubility. This approach is therefore applied to the LJ clusters optimization problem.

In a cluster, each atom is subject to a force from the other atoms, under the influence of which the atom will move. When two atoms are very close, they will repel each other; but when they are far apart, they will attract each other. In this sense, a QPS is essentially a minimization approach that makes abstract problems more concrete.

Algorithm 2
Attraction Operation.

Input: $t_{max}, step_{max}, step_{min}, X' = \{X'_1, \cdots, X'_n\}$ is the best configuration up to now, step_change is a constant less than 1.
Output: $X' = \{X'_1, \cdots, X'_n\}$ configuration of cluster after optimization.
begin
  function Attract Operation $(N;X)$
    $\varepsilon \leftarrow 1.0e-6$;
    $t \leftarrow 0$;
    $nowstep \leftarrow step_{max}$;
    Calculate E_0 using Equation(3);
    Calculate F_i using Equations (12) and (13);
    Calculate F_{total} using Equation(14);
    while $t < t_{max}$ **do**
      if $F_{total} < \varepsilon$
        break;
      end
      $i \leftarrow 0$;
      While $i < N$ **do**
        $X_i \leftarrow X_i + nowstep \times F_i$;
        $i \leftarrow i+1$;
      end
      Calculate E_1 using Equation(3) with new X;
      $t \leftarrow t + 1$;
      if $E_1 < E_0$ **then**
        $E_0 \leftarrow E_1$;
      else ($E_1 \geq E_0$ and $nowstep > step_{min}$)
        $nowstep \leftarrow nowstep \times step\_change$;
      end
      Calculate F_i using Equations (12) and (13);
      Calculate F_{total} using Equation(14);
    end
  return E_0, X;
end

For any configuration $(X_1, \cdots, X_N)\ \varepsilon\ R^{3N}$, the potential energy function of the LJ clusters is shown in Equations (1)–(3) and can also be written as Equation (10) below:

$$v(r_{ij}) = \left(\frac{1}{r_{ij}}\right)^{12} - \left(\frac{1}{r_{ij}}\right)^{6} \tag{10}$$

The potential energy function between atom i and atom j is given by Equation (11):

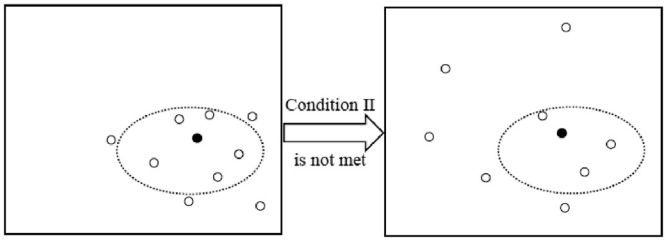

Fig. 4. Initialize particle swarm is applied of a case which the trigger condition II is not met.

$$E(r_{ij}) = 4 \times v(r_{ij}) \tag{11}$$

Therefore, the force exerted on atom i by atom j is given by Equation (12):

$$G_{ji} = -\frac{d(E(r_{ij}))}{d(r_{ij})} \times \frac{X_i - X_j}{r_{ij}} = \left(48r_{ij}^{-14} - 24r_{ij}^{-8}\right)(X_i - X_j) \tag{12}$$

where $\frac{d(E(r_{ij}))}{d(r_{ij})}$ represents the derivative function of $E(r_{ij})$.

Consequently, $(48r_{ij}^{-14} - 24r_{ij}^{-8})$ represents the size of the force, and $(X_i - X_j)$ represents the direction of the force.

The total force experienced by atom i is thus given by Equation (13):

$$F_i = \sum_{j=1, j\neq i}^{N} G_{ji} \tag{13}$$

The total force experienced by the whole cluster is given by Equation (14):

$$F_{total} = \sqrt{\frac{\sum_{i=1}^{N} F^2}{N}} \tag{14}$$

The purpose of the attraction operation is to set the total force of the whole cluster to zero. Thus, after the calculation of the force experienced by each atom, each atom moves a given step length in the direction of the force according to the magnitude of the force. The next step is to calculate the force experienced by each atom and to move every atom iteratively until the total force meets the termination condition. This strategy is substantially equivalent to the steepest descent method without linear steps. The details of the algorithm are shown in Algorithm 2.

To prevent the PSO from falling into a local optimum, we simulate a situation in which every atom in a randomly generated structure is subjected to an atomic force corresponding to that of the repulsion operation. The atomic force received in the repulsion operation is calculated by Equation (15), and the repulsion operation obeys Equation (16) below:

$$H_{i'} = G_{i'i} \tag{15}$$

$$x_{new\ i} = x_{i'} + step^{*}H_{i'} \tag{16}$$

where x_{newi} is the newly generated structure of the repulsion operation and $x_{i'} = (x_{i1'}, x_{i2'}, \ldots, x_{ih'})^T$ is a randomly generated structure of the LJ clusters. i' represents the atom corresponding to i in the randomly generated structure; the step length is set to 0.5, and each atom moves in the direction of $H_{i'}$. For each particle in the particle swarm, a new cluster structure is generated to optimize the probability that the whole particle swarm will move from the bottom of the current potential energy funnel to another funnel after the repulsion operation.

Table 2
Comparison the proposed QPS-PSO, CSO [29–31], CCPSO2 [32,33], CCDE [34,35], VLPSO-FS [19,36], HCLPSO [37], EPSO [38] and DECC-DG [39].

NAME	QPS-PSO			OTHER ALGORITHMS					
	LOWEST	AVERAGE	STD	ALGORITHM	LOWEST	AVERAGE	STD	Wilcoxon signed-rank p	SIG
LJ 7				CCDE	−1.59E+01	−1.56E+01	2.44E-01	2.E−06	*
				CCPSO2	−1.59E+01	−1.56E+01	1.68E-01	2.E−06	*
				CSO	**−1.65E+01**	−1.55E+01	4.52E-01	2.E−06	*
	−1.65E+01	**−1.65E+01**	**1.70E-08**	DECC-DG	**−1.65E+01**	**−1.65E+01**	4.32E-02	2.E−06	*
				EPSO	**−1.65E+01**	−1.64E+01	2.76E-01	1.E−01	
				HCLPSO	**−1.65E+01**	**−1.65E+01**	1.33E-02	2.E−02	*
				VLPSO-FS	−1.54E+01	−1.39E+01	1.41E+00	2.E−06	*
LJ 13				CCDE	−3.94E+01	−3.65E+01	2.79E+00	2.E−06	*
				CCPSO2	−4.11E+01	−3.87E+01	9.34E-01	2.E−06	*
				CSO	**−4.43E+01**	−4.21E+01	1.98E+00	2.E−06	*
	−4.43E+01	**−4.42E+01**	**5.21E-01**	DECC-DG	−3.43E+01	−3.16E+01	8.98E-01	2.E−06	*
				EPSO	**−4.43E+01**	−3.99E+01	1.75E+00	2.E−06	*
				HCLPSO	**−4.43E+01**	−3.99E+01	1.18E+00	2.E−06	*
				VLPSO-FS	−3.77E+01	−3.31E+01	2.25E+00	2.E−06	*
LJ 18				CCDE	−6.36E+01	−4.92E+01	1.37E+01	2.E−06	*
				CCPSO2	−6.42E+01	−6.17E+01	1.10E+00	2.E−06	*
				CSO	−6.43E+01	−6.17E+01	1.38E+00	2.E−06	*
	−6.65E+01	**−6.62E+01**	**2.74E-01**	DECC-DG	−4.16E+01	−3.67E+01	2.13E+00	2.E−06	*
				EPSO	−6.62E+01	−6.13E+01	3.00E+00	2.E−06	*
				HCLPSO	−6.55E+01	−6.06E+01	2.10E+00	2.E−06	*
				VLPSO-FS	−4.80E+01	−4.44E+01	2.35E+00	2.E−06	*
LJ 24				CCDE	−9.33E+01	−8.66E+01	3.66E+00	2.E−06	*
				CCPSO2	−9.27E+01	−8.91E+01	1.89E+00	2.E−06	*
				CSO	−8.91E+01	−8.68E+01	1.94E+00	2.E−06	*
	−9.73E+01	**−9.63E+01**	**8.16E-01**	DECC-DG	−4.97E+01	−4.33E+01	3.41E+00	2.E−06	*
				EPSO	−9.25E+01	−8.37E+01	3.72E+00	2.E−06	*
				HCLPSO	−9.08E+01	−8.37E+01	2.75E+00	2.E−06	*
				VLPSO-FS	−7.46E+01	−6.74E+01	3.39E+00	2.E−06	*
LJ 27				CCDE	−1.03E+02	−9.75E+01	2.91E+00	2.E−06	*
				CCPSO2	−1.09E+02	−1.04E+02	1.83E+00	2.E−06	*
				CSO	−1.05E+02	−1.01E+02	1.83E+00	2.E−06	*
	−1.13E+02	**−1.12E+02**	**9.54E-01**	DECC-DG	−5.14E+01	−4.74E+01	2.23E+00	2.E−06	*
				EPSO	−1.04E+02	−9.31E+01	3.74E+00	2.E−06	*
				HCLPSO	−9.79E+01	−9.44E+01	2.20E+00	2.E−06	*
				VLPSO-FS	−9.42E+01	−8.62E+01	3.31E+00	2.E−06	*
LJ 30				CCDE	−1.18E+02	−1.12E+02	3.53E+00	2.E−06	*
				CCPSO2	−1.23E+02	−1.19E+02	2.24E+00	2.E−06	*
				CSO	−1.18E+02	−1.15E+02	1.83E+00	2.E−06	*
	−1.28E+02	**−1.27E+02**	**6.67E-01**	DECC-DG	−5.30E+01	−4.76E+01	2.15E+00	2.E−06	*
				EPSO	−1.09E+02	−1.03E+02	4.35E+00	2.E−06	*
				HCLPSO	−1.18E+02	−1.08E+02	5.05E+00	2.E−06	*
				VLPSO-FS	−1.15E+02	−1.10E+02	3.06E+00	2.E−06	*
LJ 38				CCDE	−1.63E+02	−1.57E+02	3.82E+00	2.E−06	*
				CCPSO2	−1.62E+02	−1.57E+02	2.82E+00	2.E−06	*
				CSO	−1.58E+02	−1.52E+02	3.37E+00	2.E−06	*
	−1.72E+02	**−1.70E+02**	**7.97E-01**	DECC-DG	−5.90E+01	−5.13E+01	2.45E+00	2.E−06	*
				EPSO	−1.45E+02	−1.36E+02	5.90E+00	2.E−06	*
				HCLPSO	−1.46E+02	−1.39E+02	4.21E+00	2.E−06	*
				VLPSO-FS	−1.57E+02	−1.45E+02	4.19E+00	2.E−06	*
LJ 44				CCDE	−1.92E+02	−1.77E+02	1.13E+01	2.E−06	*
				CCPSO2	−1.89E+02	−1.81E+02	3.62E+00	2.E−06	*
				CSO	−1.92E+02	−1.81E+02	5.08E+00	2.E−06	*
	−2.08E+02	**−2.04E+02**	**1.82E+00**	DECC-DG	−6.12E+01	−5.77E+01	2.03E+00	2.E−06	*
				EPSO	−1.79E+02	−1.62E+02	7.59E+00	2.E−06	*
				HCLPSO	−1.71E+02	−1.60E+02	5.23E+00	2.E−06	*
				VLPSO-FS	−1.74E+02	−1.65E+02	5.63E+00	2.E−06	*
LJ 45				CCDE	−1.96E+02	−1.76E+02	2.56E+01	2.E−06	*
				CCPSO2	−1.94E+02	−1.85E+02	5.60E+00	2.E−06	*
				CSO	−1.93E+02	−1.84E+02	5.15E+00	2.E−06	*
	−2.14E+02	**−2.09E+02**	**1.61E+00**	DECC-DG	−6.35E+01	−5.97E+01	2.04E+00	2.E−06	*
				EPSO	−1.70E+02	−1.64E+02	2.80E+00	2.E−06	*
				HCLPSO	−1.72E+02	−1.64E+02	5.65E+00	2.E−06	*
				VLPSO-FS	−1.88E+02	−1.77E+02	5.64E+00	2.E−06	*
LJ 50				CCDE	−2.24E+02	−2.07E+02	1.85E+01	2.E−06	*
				CCPSO2	−2.07E+02	−1.92E+02	8.82E+00	2.E−06	*
				CSO	−2.21E+02	−2.08E+02	5.39E+00	2.E−06	*
	−2.45E+02	**−2.38E+02**	**2.41E+00**	DECC-DG	−6.67E+01	−6.16E+01	2.21E+00	2.E−06	*
				EPSO	−2.13E+02	−1.92E+02	1.11E+01	2.E−06	*
				HCLPSO	−1.96E+02	−1.85E+02	4.73E+00	2.E−06	*
				VLPSO-FS	−2.23E+02	−2.06E+02	7.52E+00	2.E−06	*
LJ 57				CCDE	−2.60E+02	5.00E+02	2.95E+03	2.E−06	*
				CCPSO2	−2.53E+02	−2.44E+02	4.40E+00	2.E−06	*
				CSO	−2.53E+02	−2.40E+02	7.33E+00	2.E−06	*

(*continued on next page*)

Table 2 (*continued*)

NAME	QPS-PSO			OTHER ALGORITHMS					
	LOWEST	AVERAGE	STD	ALGORITHM	LOWEST	AVERAGE	STD	Wilcoxon signed-rank p	SIG
	−2.83E+02	**−2.77E+02**	2.19E+00	DECC-DG	−7.23E+01	−6.78E+01	2.00E+00	2.E−06	*
				EPSO	−2.47E+02	−2.28E+02	1.44E+01	2.E−06	*
				HCLPSO	−2.20E+02	−2.14E+02	3.19E+00	2.E−06	*
				VLPSO-FS	−2.49E+02	−2.36E+02	5.97E+00	2.E−06	*
LJ 66				CCDE	−3.10E+02	8.93E+02	6.20E+03	2.E−06	*
				CCPSO2	3.45E+01	1.62E+02	6.99E+01	2.E−06	*
				CSO	−2.88E+02	−2.76E+02	8.70E+00	2.E−06	*
	−3.36E+02	**−3.32E+02**	2.63E+00	DECC-DG	−8.14E+01	−7.60E+01	2.39E+00	2.E−06	*
				EPSO	−2.88E+02	−2.69E+02	1.48E+01	2.E−06	*
				HCLPSO	−2.76E+02	−2.53E+02	9.63E+00	2.E−06	*
				VLPSO-FS	−3.24E+02	−3.02E+02	1.23E+01	2.E−06	*
LJ 69				CCDE	−3.23E+02	1.18E+04	3.69E+04	2.E−06	*
				CCPSO2	1.68E+02	3.20E+02	8.49E+01	2.E−06	*
				CSO	−3.05E+02	−2.90E+02	1.01E+01	2.E−06	*
	−3.55E+02	**−3.49E+02**	2.77E+00	DECC-DG	−8.71E+01	−7.86E+01	3.29E+00	2.E−06	*
				EPSO	−2.97E+02	−2.80E+02	1.38E+01	2.E−06	*
				HCLPSO	−2.79E+02	−2.64E+02	8.46E+00	2.E−06	*
				VLPSO-FS	−3.46E+02	−3.14E+02	1.67E+01	2.E−06	*
LJ 72				CCDE	−3.36E+02	1.65E+04	4.56E+04	2.E−06	*
				CCPSO2	4.45E+02	5.81E+02	8.21E+01	2.E−06	*
				CSO	−3.16E+02	−2.95E+02	1.67E+01	2.E−06	*
	−3.71E+02	**−3.67E+02**	**2.33E+00**	DECC-DG	−8.76E+01	−8.07E+01	2.96E+00	2.E−06	*
				EPSO	−3.29E+02	−2.97E+02	1.57E+01	2.E−06	*
				HCLPSO	−2.80E+02	−2.72E+02	4.36E+00	2.E−06	*
				VLPSO-FS	**−3.75E+02**	−3.40E+02	1.43E+01	2.E−06	*
LJ 75				CCDE	−3.54E+02	3.11E+04	7.93E+04	2.E−06	*
				CCPSO2	6.70E+02	9.78E+02	1.58E+02	2.E−06	*
				CSO	−3.29E+02	−3.04E+02	2.32E+01	2.E−06	*
	−3.91E+02	**−3.84E+02**	**2.92E+00**	DECC-DG	−9.63E+01	−8.45E+01	4.56E+00	2.E−06	*
				EPSO	−3.39E+02	−3.10E+02	1.80E+01	2.E−06	*
				HCLPSO	−3.28E+02	−2.90E+02	1.60E+01	2.E−06	*
				VLPSO-FS	**−4.13E+02**	−3.74E+02	1.65E+01	6.E−03	*
LJ 78				CCDE	−3.62E+02	8.39E+04	1.34E+05	2.E−06	*
				CCPSO2	1.07E+03	1.44E+03	1.85E+02	2.E−06	*
				CSO	−3.51E+02	−3.02E+02	5.70E+01	2.E−06	*
	−4.08E+02	**−4.03E+02**	2.77E+00	DECC-DG	−8.90E+01	−8.61E+01	2.30E+00	2.E−06	*
				EPSO	−3.58E+02	−3.35E+02	1.60E+01	2.E−06	*
				HCLPSO	−3.30E+02	−2.99E+02	1.41E+01	2.E−06	*
				VLPSO-FS	−4.01E+02	−3.74E+02	1.42E+01	2.E−06	*
LJ 83				CCDE	−3.88E+02	1.53E+05	2.55E+05	2.E−06	*
				CCPSO2	2.18E+03	2.67E+03	2.69E+02	2.E−06	*
				CSO	−3.65E+02	−3.18E+02	5.32E+01	2.E−06	*
	−4.41E+02	**−4.33E+02**	4.00E+00	DECC-DG	−8.66E+01	−8.40E+01	1.43E+00	2.E−06	*
				EPSO	−3.75E+02	−3.51E+02	1.90E+01	2.E−06	*
				HCLPSO	−3.23E+02	−3.15E+02	5.59E+00	2.E−06	*
				VLPSO-FS	**−4.41E+02**	−4.11E+02	1.73E+01	5.E−06	*
LJ 85				CCDE	−4.01E+02	3.15E+04	1.23E+05	2.E−06	*
				CCPSO2	2.62E+03	3.36E+03	4.75E+02	2.E−06	*
				CSO	−3.74E+02	−2.81E+02	8.21E+01	2.E−06	*
	−4.53E+02	**−4.45E+02**	**4.51E+00**	DECC-DG	−9.97E+01	−8.91E+01	4.72E+00	2.E−06	*
				EPSO	−3.97E+02	−3.71E+02	1.46E+01	2.E−06	*
				HCLPSO	−3.38E+02	−3.24E+02	6.43E+00	2.E−06	*
				VLPSO-FS	**−4.73E+02**	−4.42E+02	2.11E+01	6.E−01	
LJ 91				CCDE	−4.22E+02	3.47E+05	5.64E+05	2.E−06	*
				CCPSO2	4.77E+03	5.71E+03	5.85E+02	2.E−06	*
				CSO	−3.89E+02	4.02E+02	3.63E+03	2.E−06	*
	−4.89E+02	**−4.82E+02**	3.89E+00	DECC-DG	−9.42E+01	−8.79E+01	3.21E+00	2.E−06	*
				EPSO	−4.35E+02	−3.98E+02	1.98E+01	2.E−06	*
				HCLPSO	−3.84E+02	−3.58E+02	1.37E+01	2.E−06	*
				VLPSO-FS	**−5.16E+02**	−4.78E+02	2.11E+01	3.E−01	
LJ 98				CCDE	−4.47E+02	9.05E+05	1.15E+06	2.E−06	*
				CCPSO2	8.79E+03	1.06E+04	8.60E+02	2.E−06	*
				CSO	−4.27E+02	1.03E+04	3.42E+04	2.E−06	*
	−5.36E+02	**−5.24E+02**	**4.62E+00**	DECC-DG	−1.04E+02	−9.40E+01	5.60E+00	2.E−06	*
				EPSO	−4.61E+02	−4.31E+02	1.59E+01	2.E−06	*
				HCLPSO	−3.99E+02	−3.84E+02	1.02E+01	2.E−06	*
				VLPSO-FS	**−5.43E+02**	−5.05E+02	1.37E+01	2.E−05	*

The statistical comparison is performed using a Wilcoxon signed-rank test with $\alpha = 0.05$.

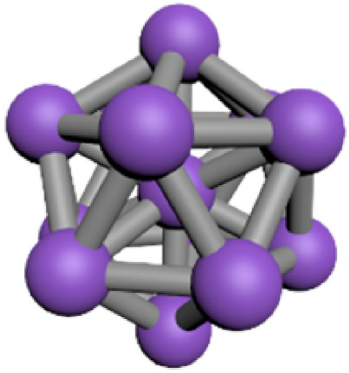

Fig. 5. The cluster structure of LJ13 obtained by QPS-PSO.

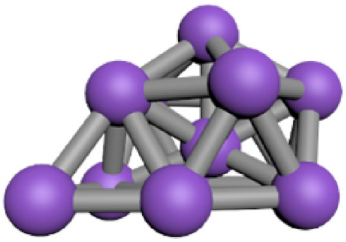

Fig. 6. The cluster structure of LJ13 obtained by CCPSO2.

4. Experiment and results

4.1. Experimental setting

We present numerical results to support our claim that QPS-PSO, in targeting the key characteristic of LJ clusters optimization, is effective at solving the LJ clusters optimization problem. For different LJ clusters, it is determined whether the zero-total force on the cluster of the attraction operation improves the location of a potential energy point. Then, it is determined whether the dispersion process of the repulsion operation plays a role in preventing descent into a local optimum as well as how great an influence the dispersion process has on the stability of the experimental results. To provide a comparison with other typical algorithms for multimodal and large-scale optimization problems, the results are compared with the latest results in terms of their numerical values and standard deviation.

In our experiment, 20 cluster systems are used for testing, including LJ7, LJ13, LJ18, LJ24, LJ27, LJ38, LJ44, LJ45, LJ50, LJ57, LJ66, LJ69, LJ72, LJ78, LJ83, LJ91 and LJ98. LJ7, LJ13, LJ18, LJ24, and LJ30 are simple systems, while LJ38 has a nontrivial double-funnel energy field [28], which is difficult to optimize. LJ83, LJ85, LJ91, and LJ98 (dimensions 230–300) are examples of large systems at high dimensions.

We compare the performance of the proposed algorithm with that of seven existing state-of-the-art algorithms: the competitive swarm optimizer (CSO) [29–31], the cooperatively coevolving particle swarm optimizer (CCPSO2) [32,33], cooperative coevolution with differential grouping (CCDE) [34,35], variable-length particle swarm optimization for feature selection (VLPSO-FS) [19,36], heterogeneous comprehensive learning particle swarm optimization (HCLPSO) [37], ensemble particle swarm optimization (EPSO) [38] and cooperative coevolution with differential optimization (DECC-DG) [39]. The maximum number of evaluations for all algorithms is set at 10^6 to ensure that there are enough for the particle swarm of each algorithm to be convergent. The particle swarm sizes are all set to $NP = 30$. The running cycle τ of the QPS is set to 100, and the threshold constant k in condition II is 0.1 [40,41]. Furthermore, the results were analyzed by the Wilcoxon signed-rank test and average Friedman Rank test [42].

4.2. Experimental results

As shown in Table 2, each algorithm runs 30 times on different numbers of atoms, and the lowest potential energies obtained in each execution are investigated. The results are analyzed using a Wilcoxon signed-rank test with $\alpha = 0.05$ [32]. They indicate that the proposed QPS-PSO performs much better than the other seven algorithms. Table 2 shows data from the statistical analysis of the experiment. The measures used in Table 2 are as follows:

(1) - LOWEST: The potential energy over 30 executions.
(2) -AVERAGE: The average potential energy over 30 executions.
(3) -STD: The standard deviation over 30 executions.
(4) -SIG: If there is a significant difference from QPS-PSO in the algorithm, then Sig is "*"; otherwise, Sig is empty.

The experimental results are presented in Table 2, which shows the lowest and mean of potential energy, and the standard deviation obtained by QPS-PSO and by CCPSO2, CCDE, CSO, VLPSO-FS, EPSO, HCPSO and DECC-DG during 30 executions. In Table 2, the best results in

Table 3
Comparison average Friedman Rank of 8 algorithms in 20 cluster systems.

NAME	QPS-PSO	CCDE	CCPSO2	CSO	DECC-DG	EPSO	HCLPSO	VLPSO-FS
LJ7	**2.07**	5.68	6.02	6.20	3.20	2.48	2.42	7.93
LJ13	**1.00**	5.90	4.67	2.57	7.70	3.60	3.57	7.00
LJ18	**1.00**	6.00	3.30	3.60	7.80	3.57	3.97	6.77
LJ24	**1.00**	3.77	2.57	3.63	8.00	5.00	5.03	7.00
LJ27	**1.00**	4.13	2.27	3.03	8.00	5.47	5.17	6.93
LJ30	**1.00**	4.43	2.17	3.37	8.00	6.53	5.50	5.00
LJ38	**1.00**	2.77	2.63	3.80	8.00	6.67	6.23	4.90
LJ44	**1.00**	3.53	2.87	3.20	8.00	5.83	6.33	5.23
LJ45	**1.00**	3.80	3.17	3.27	8.00	6.27	6.17	4.33
LJ50	**1.00**	2.90	5.43	3.30	8.00	5.43	6.33	3.60
LJ57	**1.00**	4.10	3.03	3.87	7.87	5.20	6.53	4.40
LJ66	**1.00**	3.90	7.90	4.10	6.90	4.43	5.53	2.23
LJ69	**1.00**	3.97	7.83	3.93	6.83	4.57	5.47	2.40
LJ72	**1.07**	4.83	7.73	4.13	6.70	4.10	5.50	1.93
LJ75	**1.23**	4.70	7.80	4.17	6.80	4.33	5.13	1.83
LJ78	**1.00**	5.57	7.60	4.57	6.60	3.57	5.10	2.00
LJ83	**1.07**	5.33	7.63	4.33	6.60	3.80	5.27	1.97
LJ85	**1.43**	4.20	7.93	5.27	6.90	3.53	5.17	1.57
LJ91	**1.37**	5.87	7.53	5.43	6.43	3.27	4.47	1.63
LJ98	**1.10**	6.50	7.27	5.50	6.07	3.13	4.53	1.90
Average	**1.12**	4.59	5.37	4.06	7.12	4.54	5.17	4.03

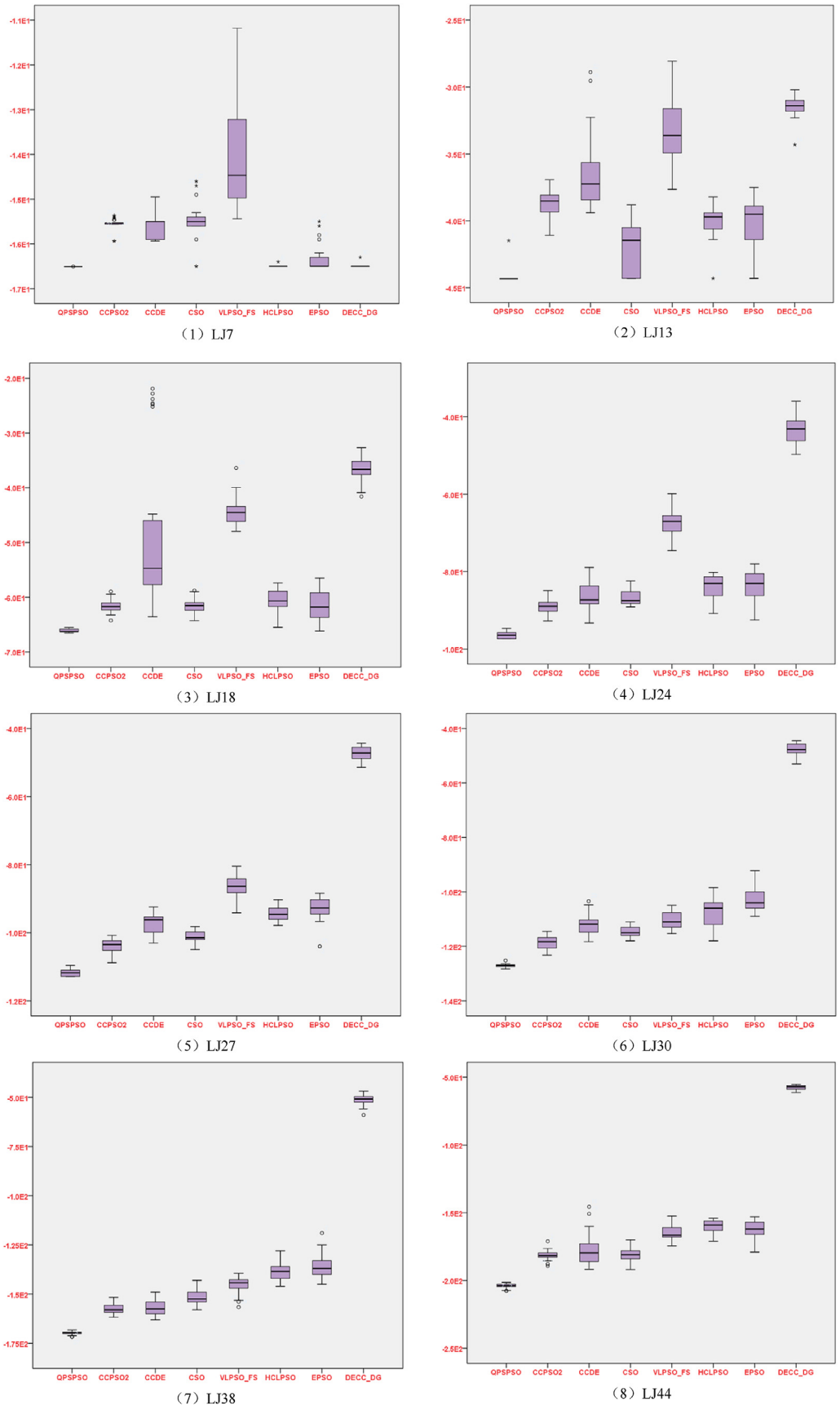

Fig. 7. Box plots of the results from 30 runs for LJ systems (1)–(20). The bars in black are the median results.

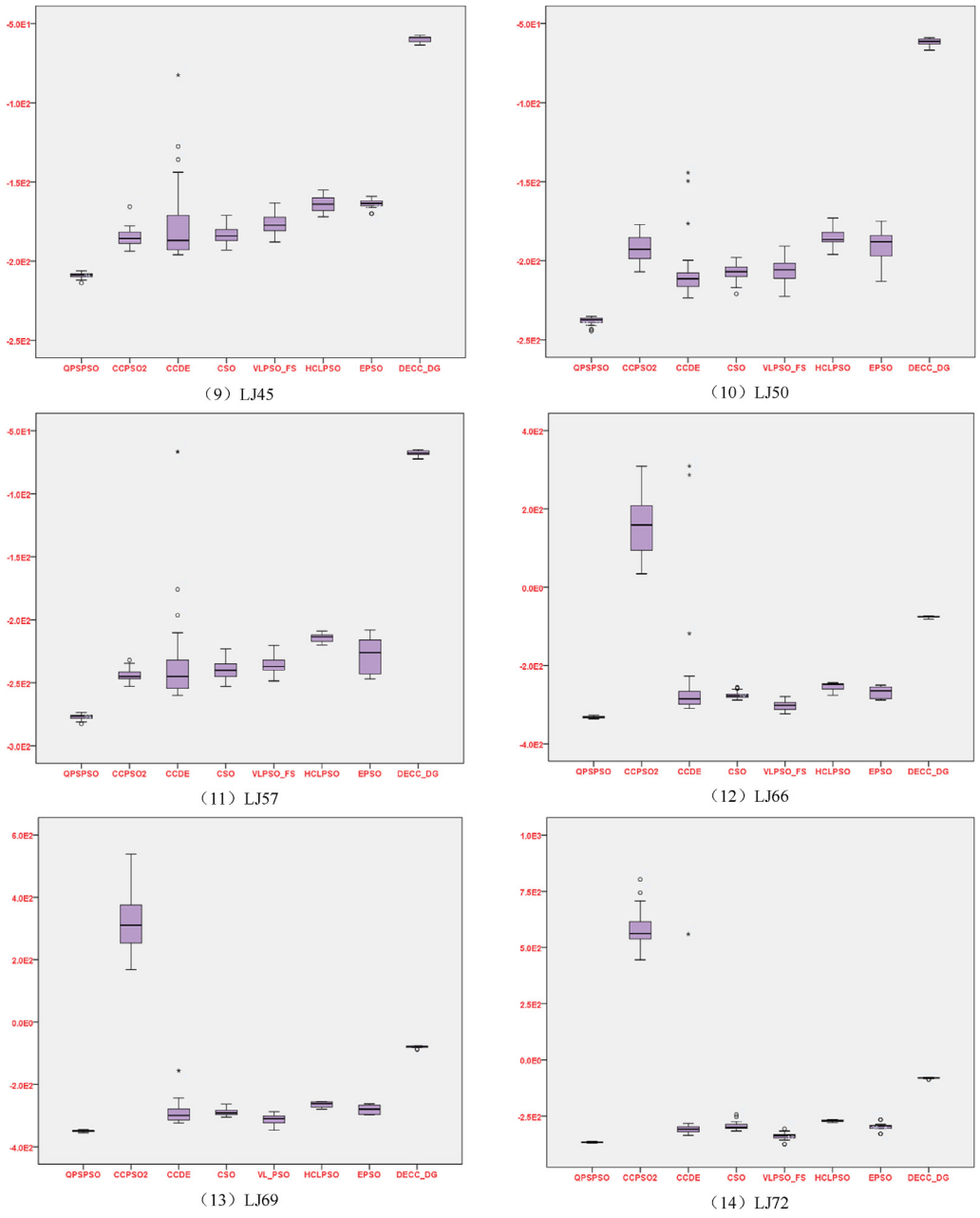

Fig. 7. (*continued*).

each instance are highlighted. It shows that the solutions obtained by QPS-PSO for all test systems are superior to those obtained by the other seven algorithms; the average potential energy and standard deviation obtained by QPS-PSO are lower than those obtained by the other seven algorithms. In terms of the lowest value, only LJ72, LJ75, LJ85, LJ91 and LJ98 are slightly higher than in VLPSO-FS, but the average value and standard deviation are lower than those of VLPSO-FS, CSO, VLPSO-FS, EPSO and HCLPSO perform relatively well in high dimensions, while the CCPSO2, CCDE and DECC-DG lose their effectiveness in LJ69 and larger systems and in LJ72 and larger systems, respectively.

To more intuitively reveal the minimum potential energy value corresponding to the LJ clusters. The LJ13 cluster is chosen for analysis and compare with other LJ clusters with different atomic numbers. This cluster has a low atomic number and yields a local minimum of relatively moderate size, while LJ clusters with higher atomic numbers cannot necessarily locate the global optimum because the number of local minimum-value points increases exponentially.

Thus, if the atomic number is smaller than that of the atoms in the LJ13 cluster, too few local minimum points are present, meaning that the results of each algorithm are too similar to show an algorithm contrast effect. Images of the clusters structure obtained by QPS-PSO and CCPSO2 for LJ13 are shown in Figs. 5 and 6. The results obtained by QPS-PSO, CSO, HCLPSO and EPSO are all −44.3268, which is currently the minimum known potential energy value for LJ13. The best result of CCPSO2 is −41.0804, which is a local minimum of LJ13. The cluster structure in Figs. 5 and 6 show that even though the difference in potential energy between the two clusters is small, the difference in structure is large. This clustering structure increases the possibility of the algorithm producing a local optimum.

Table 3 shows the average Friedman Rank of the eight algorithms over all 20 cluster systems by using the Friedman test [42]. When we calculate the average Friedman Rank, the same accuracy values for these methods are considered, and in the case of a tie, both are assigned the average value. The results of each row in Table 3 indicate that QPS-PSO

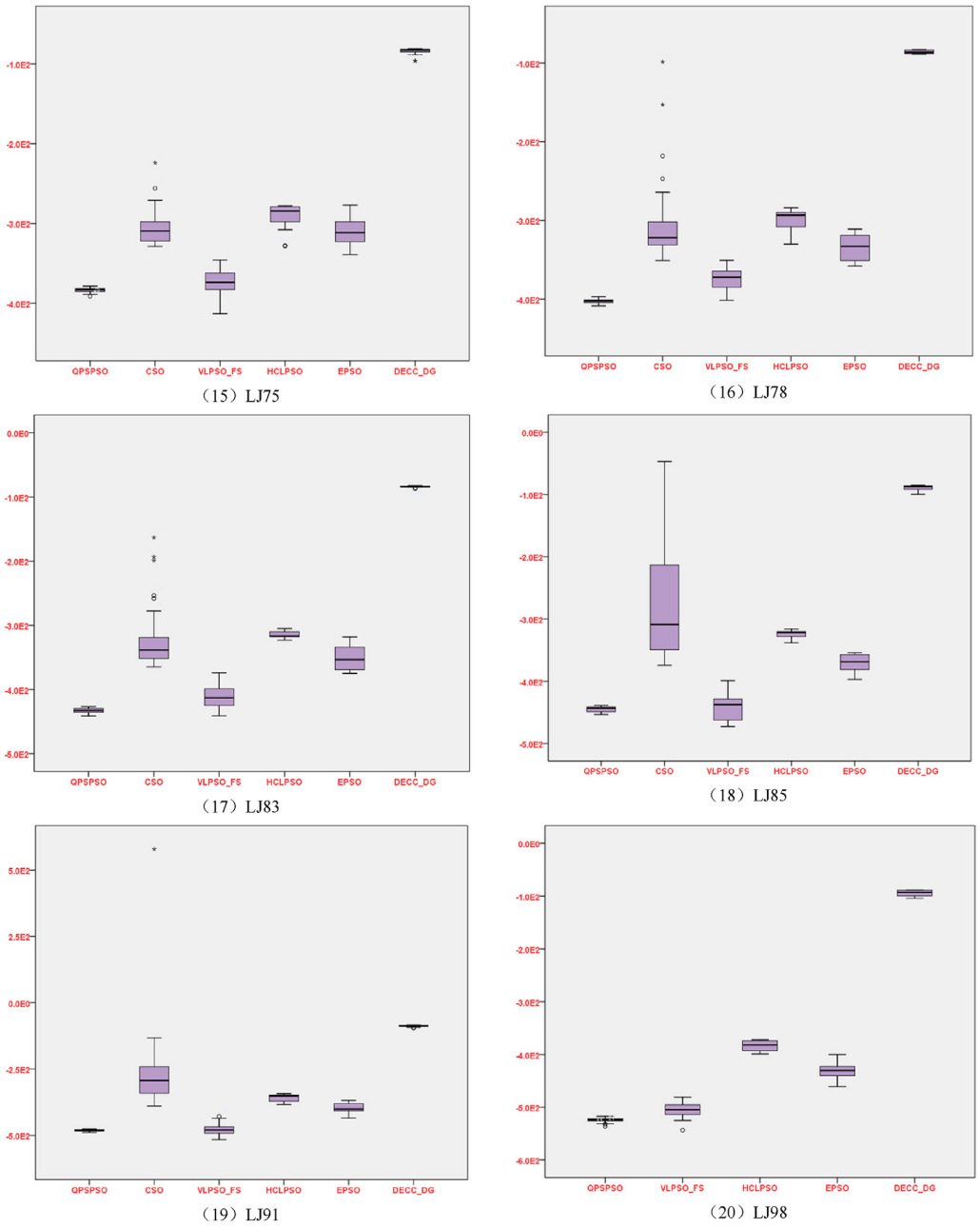

Fig. 7. (*continued*).

has the best rank.

Fig. 7 shows a box plot of the steady performance of the proposed QPS-PSO compared with that of the CCPSO2, CCDE, CSO, VLPSO-FS, EPSO, HCLPSO and DECC-DG. QPS-PSO is the most effective among all of the systems, which is verified by the mean, maximum, minimum and median of potential energy obtained in 30 executions. Because the minimum potential value obtained by some algorithms is too large compared with the minimum potential value obtained by other algorithms, the comparison in the box plot is not intuitive. Therefore, we discard the potential value obtained by CCDE and CCPSO2 after the LJ72 cluster and the potential value obtained by the CSO at the LJ98 cluster in the box plot.

4.3. Analysis of the results

Three conclusions can be drawn from the results above.

First, the data in Table 2 shows that the lowest potential energy of QPS-PSO is lower than those of the CCPSO2, CCDE, CSO, VLPSO-FS, EPSO, HCLPSO and DECC-DG in most cases. When the cluster atom is below LJ13, the results of each algorithm are similar. And QPS-PSO, CSO, EPSO, HCLPSO can obtain similar minimum values. This is related to the dispersion process of the repulsion operation. When the clustering is small, the clustering structure is relatively simple, and each algorithm can obtain reliable results. The effect of the attraction operation and repulsion operation is not obvious, and the continuous dispersion of the particle swarm has little effect on the stability of the algorithm.

However, as the number of atoms of cluster continues to increase, the cluster structure becomes increasingly complex, the attraction and repulsion operations become increasingly obvious, and the effect of scattering particles gradually weakens. Between LJ18 and LJ75, the results of QPS-PSO are the best of all the algorithms. In the middle and high dimension clusters after LJ78, the QPS-PSO, VLPSO-FS, EPSO and HCLPSO algorithms have considerable advantages over the traditional algorithms. Although the lowest potential energy value of VLPSO in

Table 4
Wilcoxon signed-rank test based statistical comparison of the 8 algorithms.

	QPS-PSO	
	W-D-L	Statistical results
CCDE	20-0-0	+
CCPSO2	20-0-0	+
CSO	20-0-0	+
EPSO	19-1-0	+
DECC-DG	20-0-0	+
HCLPSO	20-0-0	+
VLPSO-FS	18-2-0	+

Table 5
Scoring rules of "W-D-L".

Mean value	Standard deviation	Wilcoxon signed-rank p	W-D-L
A = B	A > B		L
	A < B	p<0.05	W
		p>0.05	D
A < B	A<B		W
	A>B	p<0.05	W
		p>0.05	D
A > B	A < B	p<0.05	D
		p>0.05	L
	A > B		L

A and B represent the corresponding values obtained by two different algorithms, and p represents the value of the Wilcoxon signed-rank p between A and B.

LJ78, LJ85 and LJ91 is slightly better than that of QPS-PSO, the difference between the two is not large. The reason may be that when dealing with large-scale complex problems, the attraction operation may not be able to find the point where the total force is 0 within the specified time but can only find a structure close to 0, and this affects the result. However, when combining the average potential energy value and the variance of each algorithm in a high-dimensional field, this effect is slight. For larger LJ98 cluster, the QPS-PSO algorithm can still obtain the best result by searching for structures with a total force close to 0. The comprehensive performance of QPS-PSO in higher dimensions is still the best, so it has an absolute advantage in dealing with large-scale problems. Compared with other algorithms, QPS-PSO has better stability and search capability. The above analysis shows that when the LJ clusters optimization problem is multimodal, a stable local optimal solution can be found with the attraction operation.

It is worth mentioning that LJ38 is difficult to optimize because it has a non-trivial double funnel field. As shown in Fig. 7, the box plot of the QPS-PSO algorithm is obviously superior to that of the other algorithms. Table 2 shows that the standard deviation of the CSO increased suddenly, but the standard deviation of QPS-PSO increased slightly when applied to LJ38, which indicates the stable performance of QPS-PSO.

The Wilcoxon signed-rank test is carried out for QPS-PSO and seven other algorithms. A total of 140 comparative tests were conducted in 20 clusters, and the Wilcoxon signed-rank test p values were less than significant index to 0.05. Only 3 times were higher than 0.05. This illustrates that the QPS-PSO algorithm results and those of the other seven algorithms show significant differences in most cases. Through further comparison of the median and average, supporting QPS-PSO in most cases, the results are seen to be significantly better than those of the other algorithms.

Additionally, as shown in Table 3, the average Friedman Rank of QPS-PSO is lower than that of the other algorithms in 20 cluster systems, and the total average of 20 systems is only one-quarter that of the second-place algorithm. It is proved again that the performance of the QPS-PSO algorithm is better than that of the other algorithms in each system.

The results of the QPS-PSO, CCPSO2, CCDE, CSO, VLPSO-FS, EPSO, HCLPSO and DECC-DG algorithms are compared in Fig. 7. In most cases, the maximum, minimum, median, one quarter and three quarters values in the box plot of QPS-PSO are generally closer than those of the other algorithms, indicating that the QPS-PSO algorithm has strong stability. The mean value and standard deviation of the results of the QPS-PSO algorithm in medium and high dimensions are generally better than those of the other algorithms, which indicate that the QPS-PSO algorithm is very effective. During the attraction operation, the local minimum value of the selected target point is determined by judging whether the resultant force of the cluster is zero, so that the local minimum output of the QPS-PSO algorithm is smaller than that of the other algorithms in each iteration. The algorithm prevents the particle swarm from falling into a local optimum through multiple scatterings and secondary searches of the particle swarm.

Thus, the proposed QPS framework and approach can enhance the performance of the algorithm on a large scale and with a multimodal problem. Moreover, the proposed algorithm is more efficient than the CCPSO2, CCDE, CSO, VLPSO-FS, EPSO, HCLPSO and DECC-DG for LJ clusters optimization.

4.4. Overall comparisons among the eight algorithms

In this section, we compare the overall performance of the QPS introduced in this paper with that of the seven algorithms on 20 cluster systems [42]. For brevity, we present the overall performance results of the eight algorithms in Table 4.

"+" indicates that the method in the corresponding row is statistically better than the method in the corresponding column. In contrast, "-" indicates that the method in the corresponding row is statistically worse than the method in the corresponding column. "W-D-L" indicates the "win-draw-lose" numbers for QPS-PSO versus the other algorithms.

We use a Wilcoxon signed-rank test to determine the significance among each pair chosen from the eight algorithms, as suggested in Ref. [42]. Moreover, the "W-D-L" indexes in Table 4 are obtained with reference to the mean value, standard deviation and Wilcoxon signed-rank p value and according to the rules in Table 5. We follow a similar procedure as in Refs. [42] and report the comparison in Table 3. One can see from the tables that QPS-PSO is statistically better than all other seven algorithms.

5. Conclusion

In this study, an algorithm combining PSO with a QPS is introduced to solve the LJ cluster optimization problem; the QPS is used to enhance the performance of PSO. The operations of interatomic attraction and interatomic repulsion are designed to help the particle swarm find and escape from local minima. The experimental results show that the proposed algorithm is able to find a lower potential energy than the CCPSO2, CCDE, CSO, VLPSO-FS, EPSO, HCLPSO and DECC-DG, especially in high dimensions.

In addition, there is a low standard deviation of the runs in QPS-PSO, which means that the repulsion operation is effective at forcing the result out of local minima and thereby yields results closer to the global minimum. Our statistical comparison of various algorithms shows that QPS-PSO outperforms the CCPSO2, CCDE, CSO, VLPSO-FS, EPSO, HCLPSO and DECC-DG in the LJ cluster optimization problem. Hence, we can conclude that the QPS-PSO deals effectively with the key characteristics of LJ clusters optimization in which includes multimodality and large scale. Thus, the QPS-PSO is an effective algorithm for solving the LJ cluster optimization problem.

Declaration of competing interest

None.

CRediT authorship contribution statement

Guizhen Mai: Conceptualization, Methodology. **Yinghan Hong:**

Data curation, Writing - original draft, Software. **Shen Fu:** Visualization, Investigation. **Yingqing Lin:** Writing - review & editing. **Zhifeng Hao:** Supervision. **Han Huang:** Methodology, Validation. **Yuanhao Zhu:** Software.

Acknowledgment

This work is supported by National Natural Science Foundation of China (61976052, 61876207, 61973092), Natural Science Funds for Distinguished Young Scholar of Guangdong, China (2014A030306050), Science and Technology Planning Project of Guangdong Province, China (2017A040405063, 2015B090922014, 2017B030307002, 2016B030306002, 2019B101001021), Doctor starting fund of Hanshan normal university, China (QD20190628), scientific research talents fund of Hanshan normal university, China (Z19113), International Cooperation Project of Guangzhou, China (201807010047), science and technology project of Guangzhou, China (201802010007, 201804010276) and Key Area R&D Program of Guangdong Province, China (2018B010109003). Finally, thanks to Chenyang Chao for his contribution to the preliminary research and experimental design of this paper.

References

[1] H. Li, X. Tian, X. Luo, et al., Heteroborospherene clusters Nin ∈ B40 (n = 1–4) and heteroborophene monolayers Ni2 ∈ B14 with planar heptacoordinate transition-metal centers in η7-B7 heptagons, Sci. Rep. 7 (2017) 5701–5732, https://doi.org/10.1038/s41598-017-06039-9.

[2] R. Gong, L. Cheng, Anisotropy effect of multi-center Lennard-Jones molecular clusters, Comput. Theor. Chem. 1082 (2016) 41–48, https://doi.org/10.1016/j.comptc.2016.03.008.

[3] Z. Chen, W. Jia, X. Jiang, et al., Sgo: A fast engine for ab initio atomic structure global optimization by differential evolution, Comput. Phys. Commun. 219 (2017) 35–44, https://doi.org/10.1016/j.cpc.2017.05.005.

[4] D.J. Wales, H.A. Scheraga, Global optimization of clusters, crystals, and biomolecules, Science 285 (5432) (1999) 1368–1372, https://doi.org/10.1126/science.285.5432.1368.

[5] W. Bai, L. Chen, K. Chen, D. Han, C. Tian, H. Wang Pias, Practical information-agnostic flow scheduling for commodity data centers, IEEE/ACM Trans. Netw. 25 (4) (2017) 1954–1967, https://doi.org/10.1109/TNET.2017.2669216.

[6] F.L. Custdio, H.J.C. Barbosa, L.E. Dardenne, A multiple minima genetic algorithm for protein structure prediction, Appl. Soft Comput. 15 (2) (2014) 88–99, https://doi.org/10.1016/j.asoc.2013.10.029.

[7] J. Zhang, The hybrid idea of optimization methods applied to the energy minimization of (prion) protein structures focusing on the beta2-alpha2 loop, Biochem. Pharmacol. Open Access 19 (7) (2015) 2402–2425, https://doi.org/10.4173/2167-6501.1000175.

[8] J.A. Niesse, H.R. Mayne, Global optimization of atomic and molecular clusters using the space fixed modified genetic algorithm method, J. Comput. Chem. 18 (9) (2015) 1233–1244.

[9] C. Voglis, P.E. Hadjidoukas, D.G. Papageorgiou, I.E. Lagaris, A parallel hybrid optimization algorithm for fitting interatomic potentials, Appl. Soft Comput. J. 13 (12) (2013) 4481–4492, https://doi.org/10.1016/j.asoc.2013.08.007.

[10] A.F. Ali, M.A. Tawhid, A hybrid particle swarm optimization and genetic algorithm with population partitioning for large scale optimization problems, Ain Shams Eng. J. 8 (2) (2017) 191–206.

[11] A.R. Hedar, A.F. Ali, T.H. Abdel-Hamid, Genetic algorithm and tabu search based methods for molecular 3d-structure prediction, Numer. Algebra Contr. Optim. 1 (1) (2012) 191–209.

[12] J. Lin, J. Ning, Q.L. Du, et al., Multi-agent simulated annealing algorithm based on particle swarm optimization algorithm for protein structure prediction, J. Bionanoscience 7 (1) (2013) 84–91, https://doi.org/10.1166/jbns.2013.1086.

[13] X. Shao, L. Cheng, W. Cai, An adaptive immune optimization algorithm for energy minimization problems, J. Chem. Phys. 120 (24) (2004) 11401–11406, https://doi.org/10.1063/1.1753257.

[14] J. Kennedy, R. Eberhart, Particle swarm optimization, IEEE international conference on neural networks, Proceedings (4) (1995) 1942–1948, https://doi.org/10.1109/ICNN.1995.488968.

[15] C. Xu, H. Huang, L. Lv, An adaptive convergence speed controller framework for particle swarm optimization variants in single objective optimization problems, IEEE Int. Conf. Syst. Man Cybern. (2015) 2684–2689, https://doi.org/10.1109/SMC.2015.469.

[16] Y. Jia, et al., Distributed cooperative Co-evolution with adaptive computing resource allocation for large scale optimization, IEEE Trans. Evol. Comput. 23 (2) (2019) 188–202, https://doi.org/10.1109/TEVC.2018.2817889.

[17] Y. Sun, M. Kirley, S.K. Halgamuge, A recursive decomposition method for large scale continuous optimization, IEEE Trans. Evol. Comput. 22 (5) (2018) 647–661, https://doi.org/10.1109/TEVC.2017.2778089.

[18] P. Yang, K. Tang, X. Yao, Turning high-dimensional optimization into computationally expensive optimization, IEEE Trans. Evol. Comput. 22 (1) (2018) 143–156, https://doi.org/10.1109/TEVC.2017.2672689.

[19] B. Tran, B. Xue, M. Zhang, Variable-length particle swarm optimization for feature selection on high-dimensional classification, IEEE Trans. Evol. Comput. 23 (3) (2019) 473–487, https://doi.org/10.1109/TEVC.2020.2968743.

[20] J.P. Neirotti, F. Calvo, D.L. Freeman, et al., Phase changes in 38-atom Lennard-Jones clusters. I. A parallel tempering study in the canonical ensemble, J. Chem. Phys. 112 (23) (2000) 10340–10349, https://doi.org/10.1063/1.481671.

[21] C.L. Ller, I.F. Sbalzarini, Energy landscapes of atomic clusters as black box optimization benchmarks, Evol. Comput. 20 (4) (2012) 543–573, https://doi.org/10.1162/evco_a_00086.

[22] Z. Cui, X. Cai, A new stochastic algorithm to solve Lennard-Jones clusters, in: International Conference of Soft Computing and Pattern Recognition (SoCPaR), 2011, pp. 528–532, https://doi.org/10.1109/SoCPaR.2011.6089151.

[23] D. Wales, J. Doye, Global optimization by basin-hopping and the lowest energy structures of Lennard-Jones clusters containing up to 110 atoms, J. Phys. Chem. 101 (28) (1998) 5111–5116, https://doi.org/10.1021/jp970984n.

[24] N. Doraiswamy, L.D. Marks, Preferred structures in small particles, Phil. Mag. B 71 (3) (1995) 291–310, https://doi.org/10.1080/13642819508239035.

[25] J. Cheng, René Fournier, Structural optimization of atomic clusters by tabu search in descriptor space, Theor. Chem. Accounts Theor. Comput. Model. 112 (1) (2004) 7–15, https://doi.org/10.1007/s00214-003-0552-1.

[26] S. Ye, H. Huang, C. Xu, Enhancing the differential evolution with convergence speed controller for continuous optimization problems, in: Companion Publication of the 2014 Conference on Genetic and Evolutionary Computation, 2014, pp. 161–162, https://doi.org/10.1145/2598394.2598501.

[27] W. Huang, W. Li, A hopeful cnf-sat algorithm| its high efficiency, industrial application and limitation, J. Comput. Sci. Technol. 13 (1) (1998) 9–12, https://doi.org/10.1007/BF02946608.

[28] J.P.K. Doye, M.A. Miller, D.J. Wales, The double-funnel energy landscape of the 38-atom Lennard-Jones cluster, J. Chem. Phys. 110 (14) (1998) 6896–6906, https://doi.org/10.1063/1.478595.

[29] C. Ran, Y. Jin, A competitive swarm optimizer for large scale optimization, IEEE Trans. Cybern. 45 (2) (2014) 191–204, https://doi.org/10.1109/TCYB.2014.2322602.

[30] B.G. Kim, S.H. Bae, H. Kim, et al., DSP-based CSO cancellation technique for RoF transmission system implemented by using directly modulated laser, Optic Express 25 (11) (2017) 12152, https://doi.org/10.1364/OE.25.012152.

[31] R. Cheng, Y. Jin, A competitive swarm optimizer for large scale optimization, IEEE Trans. Cybern. 45 (2) (2014) 191–204, https://doi.org/10.1109/TCYB.2014.2322602.

[32] X. Li, X. Yao, Cooperatively coevolving particle swarms for large scale optimization, IEEE Trans. Evol. Comput. 16 (2) (2012) 210–224, https://doi.org/10.1109/TEVC.2011.2112662.

[33] P. Chen, Q. Hui, Epsilon-constrained CCPSO with different improvement detection techniques for large-scale constrained optimization, in: Hawaii International Conference on System Sciences, 2016, pp. 1530–1605, https://doi.org/10.1109/HICSS.2016.727.

[34] M.N. Omidvar, X. Li, Y. Mei, X. Yao, Cooperative coz-evolution with differential grouping for largescale optimization, IEEE Trans. Evol. Comput. 18 (3) (2014) 378–393, https://doi.org/10.1109/TEVC.2013.2281543.

[35] S. García, D. Molina, M. Lozano, F. Herrera, A study on the use of non-parametric tests for analyzing the evolutionary algorithms' behaviour: a case study on the CEC'2005 Special Session on Real Parameter Optimization, J. Heuristics 15 (6) (2009) 617–644, https://doi.org/10.1007/s10732-008-9080-4.

[36] X. Cai, Z. Mei, Z. Fan, A decomposition-based many-objective evolutionary algorithm with two types of adjustments for direction vectors, IEEE Trans. Cybern. 48 (8) (2018) 2335–2348, https://doi.org/10.1109/TCYB.2017.2737554.

[37] N. Lynn, P.N. Suganthan, Heterogeneous comprehensive learning particle swarm optimization with enhanced exploration and exploitation, Swarm Evol. Comput. 24 (2015) 11–24, https://doi.org/10.1016/j.swevo.2015.05.002.

[38] N. Lynn, P.N. Suganthan, Ensemble particle swarm optimizer, Appl. Soft Comput. 55 (2017) 533–548, https://doi.org/10.1016/j.asoc.2017.02.007.

[39] M.N. Omidvar, X. Li, Y. Mei, et al., Cooperative Co-evolution with differential grouping for large scale optimization, IEEE Trans. Evol. Comput. 18 (3) (2014) 378–393, https://doi.org/10.1109/TEVC.2013.2281543.

[40] H. Huang, L. Lv, S. Ye, et al., Particle swarm optimization with convergence speed controller for large-scale numerical optimization, Soft Comput. 23 (12) (2019) 4421–4437, https://doi.org/10.1007/s00500-018-3098-9.

[41] X. Cai, Y. Li, Z. Fan, Q. Zhang, An external archive guided multiobjective evolutionary algorithm based on decomposition for combinatorial optimization, IEEE Trans. Evol. Comput. 19 (4) (2015) 508–523, https://doi.org/10.1109/TEVC.2014.2350995.

[42] R. Katuwal, P.N. Suganthan, L. Zhang, Heterogeneous oblique random forest, J. Pattern Recogn. (2019), https://doi.org/10.1016/2019.107078.